ACS NANO
Cite This: ACS Nano 2019, 13, 1932−1939
www.acsnano.org

ARTICLE

High Power Density Tower-like Triboelectric Nanogenerator for Harvesting Arbitrary Directional Water Wave Energy

Minyi Xu,[†,‡,⊥] Tiancong Zhao,[†,⊥] Chuan Wang,[†] Steven L. Zhang,[‡] Zhou Li,[§] Xinxiang Pan,[†,∥] and Zhong Lin Wang*[,‡,§]

[†]Marine Engineering College, Dalian Maritime University, Dalian 116026, China
[‡]School of Materials Science and Engineering, Georgia Institute of Technology, Atlanta, Georgia 30332-0245, United States
[§]Beijing Institute of Nanoenergy and Nanosystems, Chinese Academy of Sciences, Beijing 100085, China
[∥]Guangdong Ocean University, Zhanjiang 524088, China

Supporting Information

ABSTRACT: Wave energy is one of the most available energy sources in oceans. In this work, a design of high power density triboelectric nanogenerator (TENG) based on a tower structure is proposed for harvesting wave energy from arbitrary directions. Such tower-like TENG (T-TENG) consists of multiple units made of polytetrafluoroethylene balls and three-dimensional printed arc surface coated with melt adhesive reticulation nylon film. The power generation model coupled with the kinetic model for the T-TENG is proposed and discussed. The T-TENG can effectively convert arbitrary directional wave energy into electrical energy by utilizing charged balls rolling on an optimized arc surface due to ocean wave excitation. In addition, it is found that the power density of the present T-TENG increases linearly from 1.03 W/m^3 to 10.6 W/m^3 by increasing the units from 1 to 10 in one block. This supports that the power density of the T-TENG increases proportionally with the number of units connected in parallel without rectifiers due to its distinctive mechanism and structure. Therefore, the design of T-TENG provides an innovative and effective approach toward large-scale blue energy harvesting by connecting more blocks to form T-TENG networks.

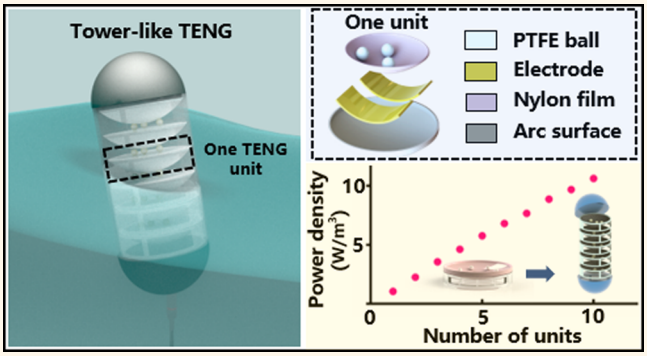

KEYWORDS: *triboelectric nanogenerator, blue energy, water wave, high power density, networks*

Due to the lack of the planet's resources and rising concerns from climate change, developing renewable and clean energy has been an imminent target for the world.[1−3] The water wave energy could turn out to be an even more benign source of power than wind, due to its abundance in the ocean, which covers more than 70% of our planet.[4] Though the potential for harvesting this energy is promising, most technologies for capturing wave power remain firmly in the testing phase.[5,6] Current devices usually have complex hydraulic or mechanical structures to harvest wave energy, and they operate by transforming the energy from the water waves into rotary motion or linear reciprocal motion for driving an electromagnetic generator.[7] However, these current ocean wave energy apparatuses exhibit unsatisfactory energy harvesting efficiency and high cost, and other methods of harvesting energy would have to be implemented.[5,8−10]

Triboelectric nanogenerators (TENGs) have been recently found to have the advantages of lightweight, low cost, and high-energy efficiency for harvesting low-frequency and irregular mechanical energy from the surrounding environment, such as from vibration, walking, wind, and water wave.[11−21] A TENG is able to generate electrical output based on contact electrification and electrostatic induction in response to an external mechanical stimuli.[9] Its fundamental physics and output characteristics can be attributed to Maxwell's displacement current.[22]

Different designs of triboelectric nanogenerators have been explored to harvest water wave energy.[1,3,9,23−30] For example, the rolling-spherical freestanding triboelectric layer-based nanogenerator fabricated by Wang *et al.* was demonstrated to harvest arbitrary directional wave energy from low-frequency water wave movements.[2] However, the screening effect from the

Received: October 29, 2018
Accepted: January 7, 2019
Published: January 7, 2019

DOI: 10.1021/acsnano.8b08274
ACS Nano 2019, 13, 1932−1939

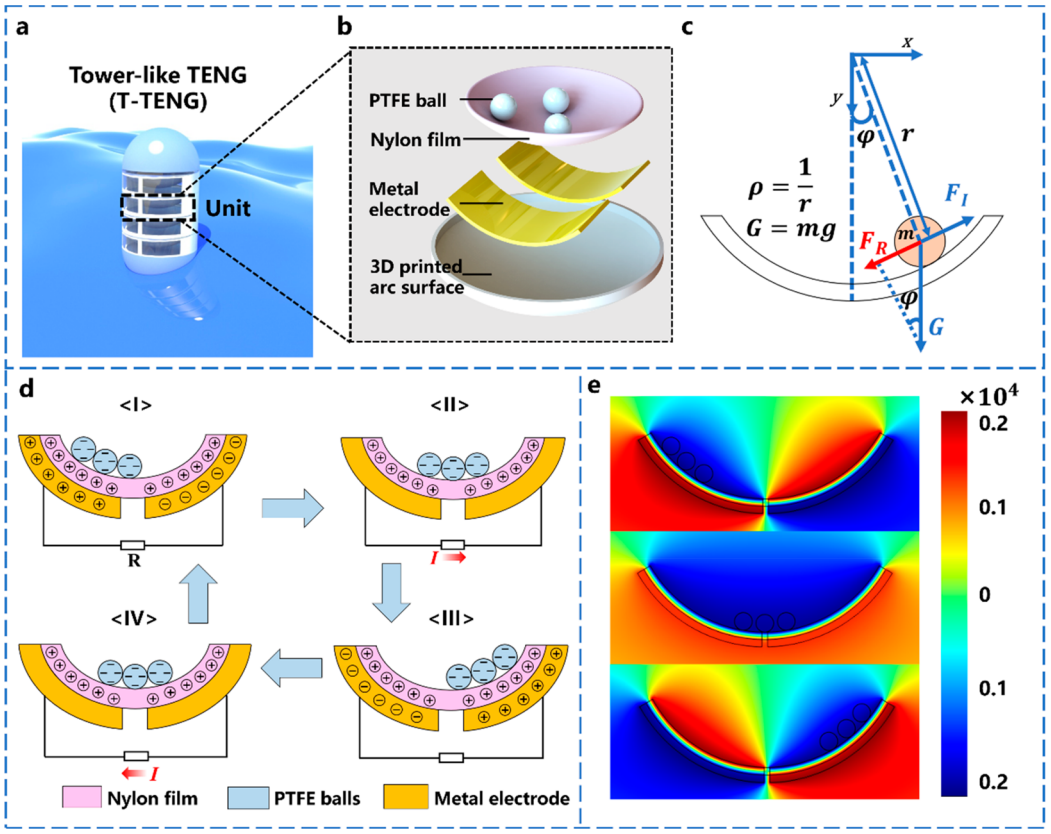

Figure 1. Structural design, basic operations, and working principles of the T-TENG. (a) Schematic diagram of the designed T-TENG consisting of multiple units. (b) The internal structure of one unit and the nylon film coated on the 3D printed arc surface. (c) Schematic diagram of dynamic analysis of a PTFE ball rolling on arc surface. (d) The working principle of the TENG unit and the charge distributed in different stages. (e) The corresponding potential distribution calculated by COMSOL in a two-dimensional plane.

charges of the ionic ocean salt water has a negative effect on the performance of TENG. Zhang *et al.*[19] addressed the problem by designing a sea snake structure-based TENG with an air gap that can minimize electrostatic induction from ions in seawater and solve the effect of dielectric screening from the water. But such TENGs cannot harvest arbitrary directional wave energy. Furthermore, for the application of water wave energy scavenging, TENG networks are required for large-scale energy harvesting.[1,7] It is worth noting that in the previous, each unit in the TENG network has to be rectified first and then connected in parallel because the network does not necessarily have the same phase.[1] Each silicon-based rectifier is found to decrease the measured voltage by 1−2 V owing to the threshold of device operation, then the power becomes lower relative to the TENG unit without a rectifier.[7]

In this work, a tower-like triboelectric nanogenerator (T-TENG) is designed and systematically investigated. The T-TENG consists of multiple units in one block, and each unit is made of polytetrafluoroethylene (PTFE) balls and a three-dimensional (3D) printed arc surface coated with melt adhesive reticulation nylon film. The power generation model coupled with the kinetic model for the T-TENG is proposed. The T-TENG can be fully packed in one block to harvest arbitrary directional wave energy and solve the effect of humidity and dielectric screening at the same time. More importantly, the power density of the T-TENG is found to increase proportionally with the number (N) of units connected in parallel without rectifiers in one block. Therefore, the design of T-TENG can provide an innovative and effective approach toward large-scale blue energy harvesting by connecting more blocks to form T-TENG networks.

RESULTS AND DISCUSSION

Structure and Working Principle of the T-TENG. As shown in Figure 1a,b, the T-TENG includes two main parts, the tubular block and its internal multiple units. The tubular block with the shell diameter of 100 mm is made of acrylic. Figure 1b shows a schematic diagram of the freestanding structured design that consists of PTFE balls and two stationary electrodes. The PTFE ball can roll back and forth between the two electrodes under wave excitation, which produces an alternating current to the external load. To enhance the contact electrification, PTFE balls, Kapton/Nylon dielectric film, and an aluminum electrode are used in the TENG unit. The Kapton/Nylon film (50 μm in thickness) covers the two electrodes (Al film thickness: 50 μm, size: 6 cm × 3 cm) that are taped to a 3D printed arc surface shell (diameter 94 mm, height 20 mm). The Kapton/Nylon film had been bonded to aluminum electrodes by hot pressing.[31] The detailed manufacturing process is shown in the Experimental Section. The scanning electron microscopy (SEM) image of the dielectric film is shown in Supplementary Figure S1.

The working principle of the T-TENG is shown in Figure 1c,d. Under the excitation of the external wave, PTFE balls roll back and forth on the arc surface. After multiple cycles of contact with the dielectric film, PTFE balls become negatively charged, and the charges remain on the surface because the PTFE balls are electret. When PTFE balls roll to the left, positive charges are induced on the left electrode. Then the current generates in the

DOI: 10.1021/acsnano.8b08274
ACS Nano 2019, 13, 1932−1939

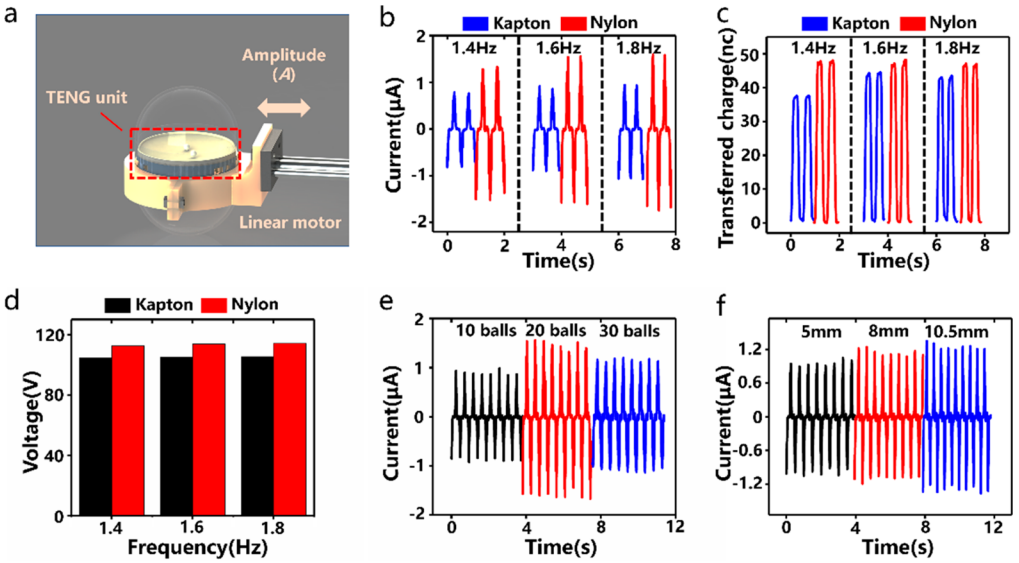

Figure 2. Effect of dielectric materials and the number and diameter of PTFE balls on electrical performance of a TENG unit. (a) Schematic diagrams of the TENG unit pushing reciprocally by the linear motor with the amplitude A = 90 mm. (b) The induced short-circuit current I_{sc}, (c) short-circuit transferred charge Q_{sc}, and (d) the open circuit voltage V_{oc} of the TENG unit for the dielectric film of Nylon and Kapton. The short circuit current output of the TENG unit for PTFE balls with (e) different numbers and (f) diameter.

loop and flows to the right electrode with PTFE balls rolling back. Under the combined action of gravity force, support force, and the damping torque, PTFE balls can periodically roll in the arc surface to produce alternating current by utilizing the freestanding mode of TENG. The COMSOL Multiphysics software based on finite-element simulation is employed to calculate the potential distribution across the two electrodes at different states, as shown in Figure 1e. The potential contour clearly shows the potential difference between the two electrodes, which would drive the current flowing in the external circuit.

To obtain the dynamic and electrical model of the T-TENG, we assume that the tubular block sways in the ocean wave with its frequency and amplitude being f and A, respectively. All PTFE balls move in the same phase in one block. Thus, PTFE balls move periodically and follow the dynamic equation:

$$\ddot{\varphi} + \gamma\dot{\varphi} + (\omega_0)^2 \sin\varphi = (2\pi f)^2 \frac{A}{r}\cos(2\pi ft)\cos\varphi \tag{1}$$

where φ is the relative angle between the inertia ball and the arc surface (angular displacement), γ is the damping constant between the inertia ball and the arc surface, ω_0 is the rotation angular velocity of the inertia ball in the arc surface, and r is the radius of arc surface, as shown in Figure 1c.

The TENG can be treated as an ideal voltage source and capacitor in series; thus the differential equation for the TENG unit when the external load is pure resistance R can be obtained by Kirchhoff's law as follows:

$$R\frac{dQ}{dt} = -\frac{1}{C(\varphi)}Q + V_{oc}(\varphi) \tag{2}$$

where $V_{oc}(\varphi)$ and $C(\varphi)$ is the open circuit voltage and the capacitance, respectively, and φ is the relative rotation angle which can be obtained by solving eq 1. In this work, the T-TENG is designed with N multiple units in parallel without rectifiers.

As the amount of transferred charge Q between the two electrodes has no relation to the external resistance, the T-TENG can be also treated as an ideal current source. Thus, the current ($I_{T\text{-}TENG}$) of T-TENG with N multiple units in parallel can be N times relative to the current (I_1) of one unit because all PTFE balls can move in the same phase in one block, that is,

$$I_{T\text{-}TENG} = \sum_{i=1}^{N} I_i = NI_1 \tag{3}$$

Thus, the voltage ($V_{T\text{-}TENG}$) across the resistance (R) of the T-TENG is also found to be N times relative to the voltage (V_1) of one unit, that is,

$$V_{T\text{-}TENG} = I_{T\text{-}TENG}R = NI_1R = \sum_{i=1}^{N} V_1 \tag{4}$$

Further, the power density ($P_{T\text{-}TENG}$) is obtained as the following:

$$P_{T\text{-}TENG} = \frac{V_{T\text{-}TENG}I_{T\text{-}TENG}R^2}{NA_1} = \frac{N^2I_1^2R}{NA_1} = NP_1 \tag{5}$$

where A_1 is the volume, and P_1 is the power density of one TENG unit. From eq 5, it is amazing to find that the power density of the T-TENG is N times relative to that (P_1) of one unit, which is verified by our experimental results.

Performance of the T-TENG. The TENG unit consists of PTFE balls, aluminum electrodes, and a 3D printed hemisphere shell. As shown in Figure 2, the output of the TENG unit is optimized by changing the paired triboelectric materials. One option uses PTFE balls and Nylon film, and the other option adopts PTFE balls and Kapton film, as shown in Figure 2a. A linear motor was used to simulate the swaying motion of the T-TENG floating body in water waves at low frequencies (0.8 Hz < f < 2.4 Hz) with an amplitude of 90 mm. The PTFE balls move back and forth in one direction at the same frequency f. For the floating body moving at the frequency of 1.4−1.8 Hz and an amplitude of 120 mm, the peak induced short-circuit current I_{sc} of the Nylon/PTFE is 1.4 μA, which is over 2 times higher than that of the Kapton/PTFE (Figure 2b). Similarly, the short-

DOI: 10.1021/acsnano.8b08274
ACS Nano 2019, 13, 1932−1939

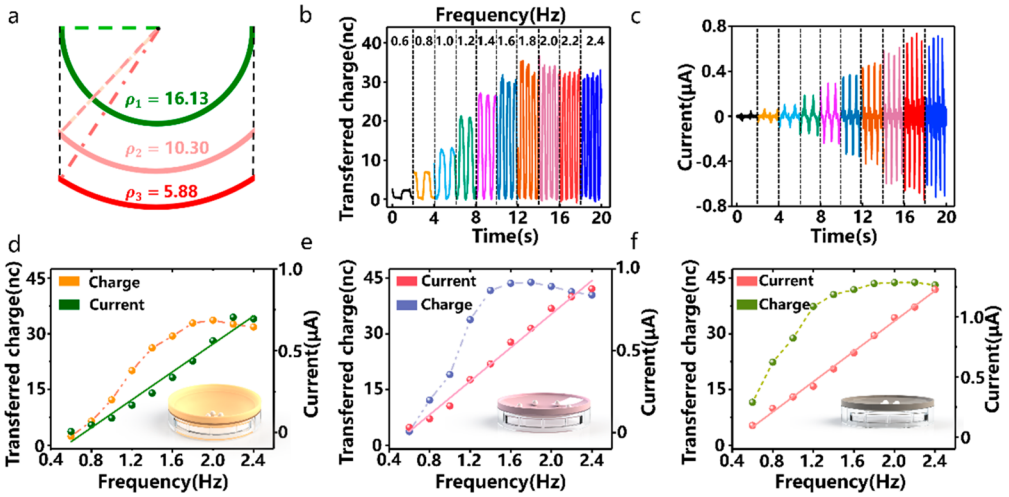

Figure 3. Electrical performance of a TENG unit with different arc surfaces. (a) The diagram of the arc surface with different curvatures. The (b) transferred charge and (c) short-circuit current of a TENG unit measured at different frequency for the arc surface curvature of ρ = 16.13 m^{-1}, that is, a hemisphere shell. The variation of transferred charge and short circuit current with frequency for the curvature (d) ρ = 16.13 m^{-1}, (e) ρ = 10.30 m^{-1}, and (f) ρ = 5.88 m^{-1}, respectively. Note that the corresponding arc surface structure is inserted in each figure.

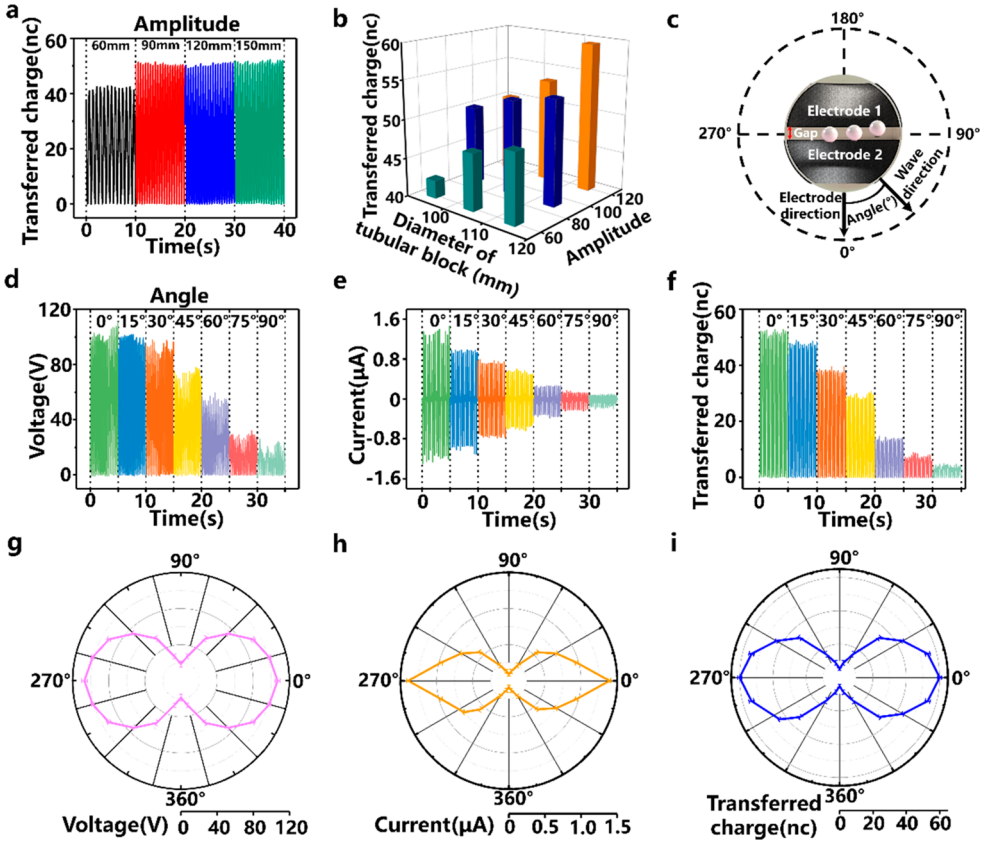

Figure 4. Electrical performance of a TENG unit with different wave amplitude and direction. (a) The transferred charge on the amplitude ranging from 60 mm to 150 mm at the constant frequency of 1.6 Hz. (b) A 3D graph of the output charge peak at different amplitude and diameter of tubular block. (c) The diagram of the angle between wave direction and electrodes direction. The dependence of (d) open circuit voltage, (e) short circuit current, and (f) transferred charge on the angle ranging from 0° to 90° with the amplitude of 120 mm. The directional map of the (g) open circuit voltage V_{oc}, (h) short-circuit transferred charge Q_{sc}, and (i) short-circuit current I_{sc}.

circuit transferred charge Q_{sc} and open circuit voltage V_{oc} of the Nylon/PTFE are also found to be higher than that of Kapton/PTFE (Figure 2c,d). The better performance of the Nylon/PTFE is believed to be caused by the most significant difference in triboelectric material series. Therefore, the PTFE balls and Nylon film are used in the following experiments.

Along with the triboelectric paired materials, the electrical performance of a TENG unit at different number n and diameter d of PTFE balls is also compared in Figure 2e,f. Since scaling the device does not change the power density, the influence of the PTFE ball's diameter and number was studied while maintaining the outer shell's diameter the same.[2] As shown in Figure 2e, for

DOI: 10.1021/acsnano.8b08274
ACS Nano 2019, 13, 1932−1939

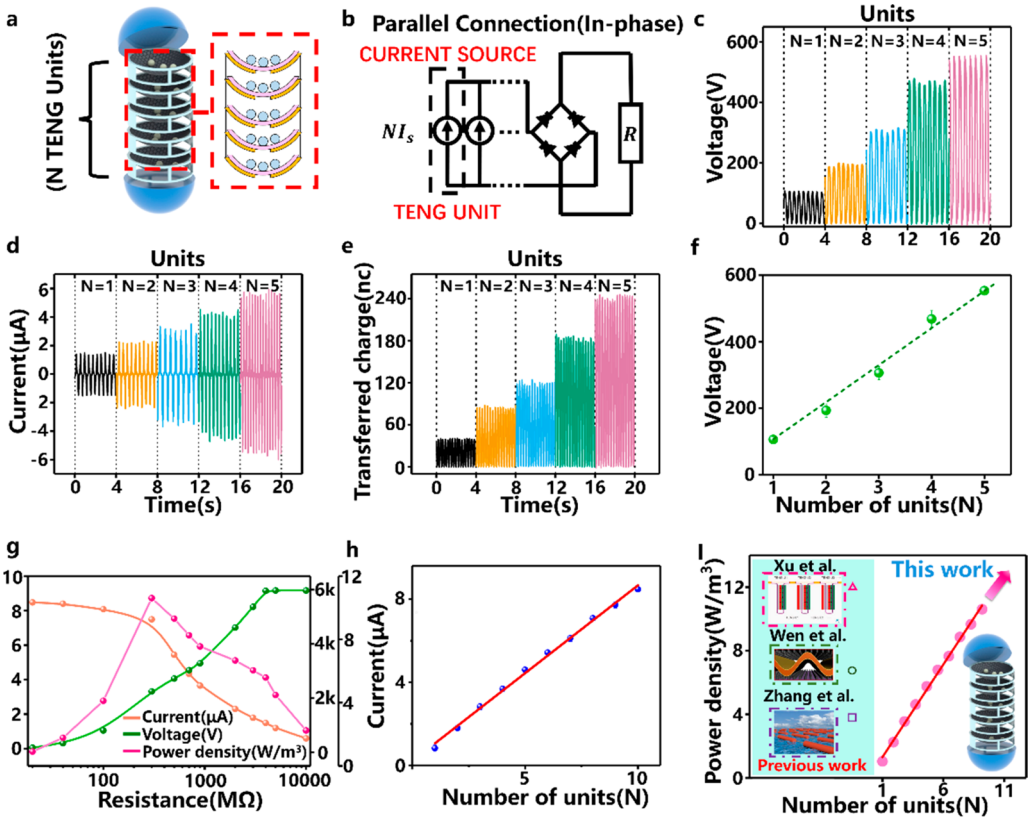

Figure 5. Output performance of the T-TENG consisting of multiple units connected in parallel in one tubular block. The diagram of (a) the T-TENG structure and (b) corresponding equivalent circuit diagram. The (c) voltage across the resistance V_R, (d) transferred charge Q_c, and (e) induced current I of the T-TENG with the number of units increasing. (f) Variation of the voltage across the resistance output of the T-TENG with the number of units. Dependence of (g) the output voltage and current and power density for T-TENG with 10 units on the resistance of the load. (h) Variation of the current, voltage, and internal resistance with the number of units. (i) Comparison of the power density of the present T-TENG and previous sea snake TENG,[19] wavy-structured TENG,[32] and air-driven membrane structure TENG.[33]

the number n of the PTFE balls varying from 10 to 30, the maximum value of the induced short-circuit current I_{sc} is found to be 1.3 μA at n = 20. It is also interesting to find that the value of I_{sc} increases from 1 μA to 1.3 μA with the diameter of the PTFE balls increasing from 5 mm to 10.5 mm. This is likely due to the increase of frequency of the balls moving due to a larger gravitational force, causing an increase in the current. Thus, the present TENG unit is made of PTFE balls with the diameter of 10.5 mm and utilizes 20 PTFE balls per layer.

In addition, the resonance phenomenon of the PTFE balls rolling on the arc surface is quite important to the output performance of the T-TENG. According to eq 1, the resonance frequency f_0 can be obtained as follows:

$$f_0 = \frac{1}{2\pi}\sqrt{\rho g} \tag{6}$$

It can be known from eq 6 that the resonant frequency f_0 of the PTFE ball rolling in the arc surface depends on the curvature ρ of arc surface. Figure 3a shows the diagram of the arc surface varying from a hemisphere shell (ρ = 16.13 m^{-1}) to a flatter shell (ρ = 5.88 m^{-1}). The output performance of the TENG unit with an arc surface (ρ = 16.13 m^{-1}) is measured by swaying the device in a linear motor at the condition of 0.6 Hz < f < 2.4 Hz and A = 90 mm. Due to the inertia effect, the PTFE balls can synchronously move at the same frequency with the linear motor, but the rolling magnitude of the PTFE balls depends on the curvature. As shown in Figure 3b, the short-circuit transferred charge Q_{sc} for the hemisphere shell increases quickly for f < 2.0 Hz and then reaches a maximum value of 35 nC at the frequency of 2.0 Hz. According to eq 6, the resonant frequency f_0 for the PTFE balls rolling in the hemisphere shell (ρ = 16.13 m^{-1}) is obtained to be 2.0 Hz. This suggests that the rolling balls have the largest magnitude at the resonant condition to produce the largest transferred charge. With further increasing f, the value of Q_{sc} decreases slowly. The peak value of induced short-circuit current I_{sc} is found to increase with the frequency (Figure 3c). The detailed variation of peak values of the Q_{sc} and I_{sc} for the hemisphere shell on the frequency is shown in Figure 3d. As shown in Figure 3d, the peak value of I_{sc} increases in the frequency range of $f \leq$ 2.2 Hz. Compared to the value obtained at f = 2.2 Hz, the peak value of I_{sc} at f = 2.4 Hz decreases by 1.2%. This may be because the higher inertial force makes the PTFE balls scatter more at higher frequency in a hemisphere shell. Also, the dependence of the output of a TENG unit on frequency for flatter arc surfaces with ρ = 10.3 m^{-1} and ρ = 5.88 m^{-1} is shown in Figure 3e,f, respectively. Note that the corresponding arc surface structure is inserted in each figure. It is interesting to find that the resonant frequency f_0 = 1.6 Hz for ρ = 10.30 m^{-1} and f_0 = 1.2 Hz for ρ = 5.88 m^{-1}. This suggests that the resonant frequency becomes lower with the arc surface having a smaller curvature. In addition, the values of Q_{sc} and I_{sc} for the smaller curvature arc surface are higher and more broadband than a device with a higher curvature arc surface. Therefore, the water wave energy can be easily harvested by utilizing a flatter arc surface.

DOI: 10.1021/acsnano.8b08274
ACS Nano 2019, 13, 1932−1939

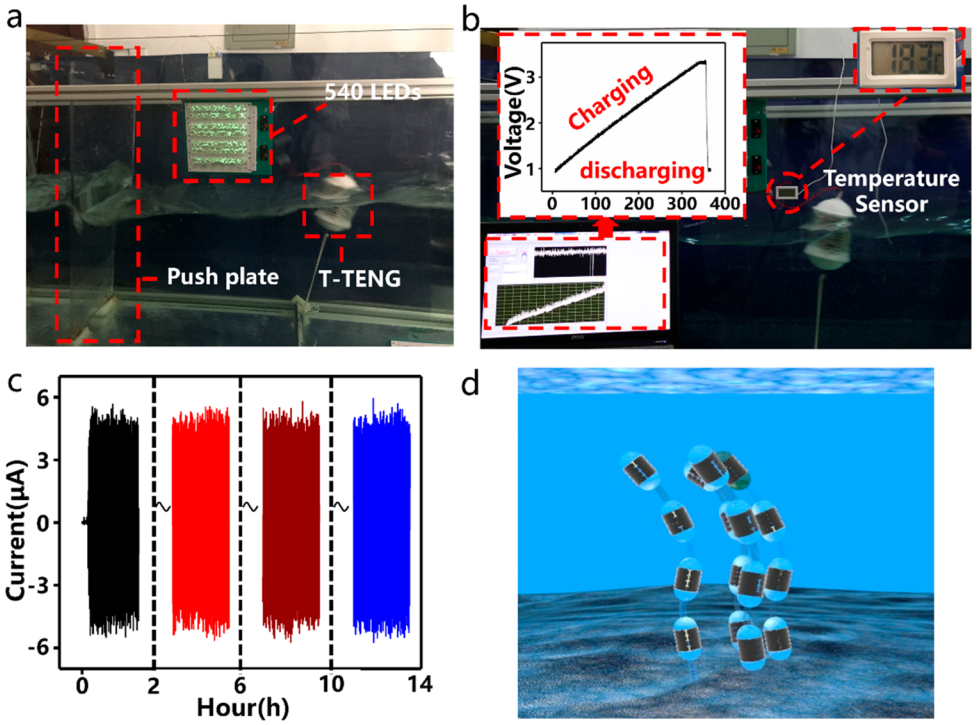

Figure 6. Application of the T-TENG with five units connected in parallel in one block for wave energy harvesting. (a) Image of 540 green LEDs lighted by the T-TENG. (b) Image of the thermometer powered by the T-TENG. The inset is the charging and discharging voltage of the capacitor. (c) The voltage of T-TENG tested in a water wave tank for 14 h. (d) T-TENG networks formed by connecting more blocks toward large-scale blue energy harvesting.

To investigate the impact of the wave amplitude (A) and direction on the electrical performance of the TENG unit, the voltage, current, and charge of the TENG unit under actuation from the linear motor with an amplitude ranging from 60 mm and 150 mm are measured. As shown in Figure 4a and Figure S2, at a constant frequency of 1.6 Hz and a diameter of the tubular block of 94 mm, the transferred charge and short circuit current are obtained for the amplitude ranging from 60 mm to 150 mm. It is found that the current increases with the amplitude increasing, because the larger amplitude produces a higher inertial acceleration of the PTFE balls (Figure S2). The charge seems to be independent of the amplitude for $A > 90$ mm, because the efficient rolling displacement of the PTFE balls reaches the maximum value, that is, the entire diameter of the tubular block. Furthermore, the transferred charge of the TENG unit was measured by varying the diameter of tubular block from 94 mm to 114 mm (Figure S3). The amplitude ranges from 60 mm to 120 mm, and the frequency is set to be 1.6 Hz. Figure 4b shows the dependence of the output transferred charge peaks on the amplitude and diameter of tubular block. It is found that the transferred charge can be enhanced by increasing the diameter of the tubular block and the amplitude. This suggests that the tubular block with larger diameter is needed to harvest water waves with higher wavelengths.

The dependence of the voltage, current, and charge of the TENG unit on the wave direction is shown in Figure 4d–i. Here, the voltage, current, and charge were measured by changing the angle between the wave direction and electrodes direction, as shown in Figure 4c. Obviously, the highest performance (V_{oc} = 105 V, I_{sc} = 1.3 μA, and Q_{sc} = 51 nC) of the TENG unit is obtained at the angle of 0°, at which the PTFE balls move parallel to the electrode direction, thus having the largest efficient displacement. With increasing the angle from 0° to 90°, the electrical performance of the TENG unit gradually decreases to a minimum (V_{oc} = 20 V, I_{sc} = 0.3 μA, and Q_{sc} = 6 nC). This is caused by the PTFE balls rolling in the center regions between the two electrodes for the angle of 90°, and the contact area between the balls and the film that is covering the electrode is not large enough, which would decrease the amount of charges transferring in the circuit. As shown in Figure 4g–i, it is worth noting that the TENG unit can harvest wave energy from arbitrary directions, even though the performance is not good enough for the angles of 90° and 270°.

To harvest wave energy more effectively, a T-TENG consisting of multiple units connected in parallel in one tubular block is designed, as shown in Figure 5a. Due to all PTFE balls moving in the same phase, it is unnecessary to utilize rectifiers for connecting units. The T-TENG can be treated as a current source and power marine sensors with just one rectifier. The equivalent circuit of the T-TENG is shown in Figure 5b. The voltage across the resistance, short-circuit current, and charge were measured with different layers connected in parallel. All three increased with increasing the number of units, as shown in Figure 5c–e. It is quite interesting to find that the voltage across the resistance V_R increases with the number of units connected in parallel without rectifiers in one block. Such observation is also found in Zhang *et al.*[19] Figure 5f shows that voltage across the resistance increases proportionally with the number of units. This is consistent with the prediction of eq 4.

Furthermore, the current I, voltage V, and power density P of T-TENG at different load resistance R with the number of units increasing from 1 to 10 is shown in Figure 5g and Figure S4. Note that the voltage is obtained by multiplying current and resistance. The power density reaches maximum value when the external resistance equals the internal impedance. Figure 5h shows that the short circuit current and voltage across the

DOI: 10.1021/acsnano.8b08274
ACS Nano 2019, 13, 1932–1939

resistance increase proportionally with increasing the number of units, while the internal impedance decreases. It is surprising to find that the power density of the T-TENG increases from 1.03 W/m^3 to 10.6 W/m^3 for the number of units increasing from 1 to 10. This is consistent with the prediction of eq 5. In previous work, Zhang *et al.*[19] designed a sea snake TENG with the power density being 3 w/m^3. Wen *et al.* invented a wavy-structured TENG with the power density being 7 w/m^3.[32] An integrated TENG array device based on air-driven membrane structures was designed by Xu *et al.*[33] to effectively harvest water wave energy, and the power density was 13.23 w/m^3. Compared to these previous works, the most significant advantage of the T-TENG is that its power density can increase with the number of units in parallel without rectifiers. It is worth noting that the power density can be further increased by utilizing more units connected in parallel without rectifiers in one block, due to all PTFE balls in one block moving in the same phase and the TENG unit being treated as a current source.

Demonstration. In the demonstration, the T-TENG consisting of five units connected in parallel in one block is utilized for harvesting wave energy in a water tank. The T-TENG is pulled by a rope to the bottom of the tank. Thus, the T-TENG can vibrate with the waves generated by a push plate. As shown in Figure 6a,b and Movie S1 and S2, the TENG can power more than 500 green LEDs. Under the wave excitation, the induced peak current I_{sc} of 5.8 μA and the transferred charge Q_c of 220 nC is shown in Figure S5. Moreover, the T-TENG can also be employed with energy storage devices to act as power sources for commercial electronic sensors. Here, a 100 μF capacitor, bridge rectifier, and a thermometer are applied. The voltage of the capacitor increases from 0 to 3.3 V in 7 min and then the thermometer was powered by the capacitor, as shown in Figure 6b. The above concepts and designs can provide feasible power solutions for long-term, large-area, on-site, and near-real-time monitoring of water parameters and may be the best power option.[2] Due to its distinctive mechanism and structure, the electrical performance of the T-TENG exhibits a quite stable state in the stability test for more than 14 h, see Figure 6c. In addition, the T-TENG shell with acrylic tube can effectively minimize the dielectric shielding of the device's performance.[19] Therefore, the design of T-TENG provides an innovative and effective approach toward large-scale blue energy harvesting by connecting more blocks in parallel to form T-TENG networks (Figure 6d).

CONCLUSION

In the present work, a design of triboelectric nanogenerator based on a tower structure is proposed and systematically investigated. Such a tower-like triboelectric nanogenerator (T-TENG) consists of multiple units made of PTFE balls and a 3D printed arc surface coated with melt adhesive reticulation nylon film. The T-TENG can effectively convert arbitrary directional and low-frequency wave energy into electrical energy by utilizing charged PTFE balls rolling on an arc surface. As all PTFE balls in one block move in the same phase and the TENG unit is treated as a current source, the power density of the T-TENG multiply increases with the number (N) of units connected in parallel without rectifiers. This is verified by our results, that is, the power density of the T-TENG increases from 1.03 W/m^3 to 10.6 W/m^3 by increasing the units N from 1 to 10 in one block. In a water wave tank, the T-TENG with 5 units in parallel can directly drive 540 LEDs and charge a 100 μF capacitor to rated voltage within several minutes. The T-TENG shell with acrylic tube can effectively minimize the dielectric shielding of the device's performance. Therefore, the design of T-TENG provides an innovative and effective approach toward large-scale blue energy harvesting by connecting more blocks to form T-TENG networks.

EXPERIMENTAL SECTION

Manufacture of the TENG Unit and T-TENG. The arc surface material is made of polylactic acid (PLA), which was produced from North Bright company. The geometric models of arc surfaces with different curvatures were prepared using the Solidworks software. Then the designed arc surfaces were printed by a 3D printer (D-Force). Two aluminum electrodes with a thickness of 50 μm and size of 6 cm × 3 cm are parallelly attached onto the inner arc surface. Furthermore, Nylon film and Kapton film with 50 μm in thickness and 7 cm × 7 cm in size are introduced to cover electrodes, respectively. The surface morphology of Nylon and Kapton films was measured using a field emission scanning electron microscope (FESEM SU 8010). The PTFE balls of various different diameters were produced by 3M company. A series of PTFE balls with diameters of 5.0, 8.0, and 10.5 mm are placed in the arc shell. Multiple units are connected in parallel to form a tower-like TENG. Finally, the T-TENG is glued inside the acrylic shell and finally sealed with epoxy paint to make it completely waterproof.

Electrical Measurement of the TENG Unit and T-TENG. To measure the electrical output of the unit and T-TENG, a programmable electrometer (Keithley Model 6514) is used. The wave simulation system of the adjustable speed motor (US-52) equipped with a reduction gearbox (5GU-5-K MAILI) was used to simulate the water wave motion. Finally, the charging and discharging performance of the T-TENG was measured using a capacitor (100 μF, 50 V) and a commercial thermometer.

ASSOCIATED CONTENT

Supporting Information

The Supporting Information is available free of charge on the ACS Publications website at DOI: 10.1021/acsnano.8b08274.

SEM image of nylon film coated on the 3D printed arc surface; short-circuit current of the TENG unit on the amplitude ranging from 60 mm to 150 mm; transferred charge of the TENG unit with the tubular block diameter; dependence of the output voltage and current and power density for T-TENG with different units on the resistance of the load; output of the T-TENG under wave excitation in a water wave tank (PDF)

Movie S1: Demonstration of the T-TENG for harvesting wave energy to power 540 LEDs (AVI)

Movie S2: Demonstration of the T-TENG for harvesting wave energy to power a thermometer (AVI)

AUTHOR INFORMATION

Corresponding Author

*E-mail: zhong.wang@mse.gatech.edu.

ORCID

Zhou Li: 0000-0002-9952-7296

Zhong Lin Wang: 0000-0002-5530-0380

Author Contributions

$^{\perp}$These authors contributed equally to this work.

Notes

The authors declare no competing financial interest.

ACKNOWLEDGMENTS

The supports of the Nature Science Foundation of China (grant nos. 51879022, 51506019), the National Key Research and

DOI: 10.1021/acsnano.8b08274
ACS Nano 2019, 13, 1932−1939

Development Program of China (no. 2016YFA0202704), the "Thousands Talents" program for pioneer researcher and his innovation team in China, the Fundamental Research Funds for the Central Universities, China (nos. 3132016337, 3132016204), and Young Elite Scientists Sponsorship Program By CAST (2016QNRC001) are gratefully acknowledged.

REFERENCES

(1) Wang, Z. L. Catch Wave Power in Floating Nets. *Nature* **2017**, *542*, 159−160.
(2) Wang, X.; Niu, S.; Yin, Y.; Yi, F.; You, Z.; Wang, Z. L. Triboelectric Nanogenerator Based on Fully Enclosed Rolling Spherical Structure for Harvesting Low-Frequency Water Wave Energy. *Adv. Energy Mater.* **2015**, *5*, 1501467.
(3) Wang, X.; Wen, Z.; Guo, H.; Wu, C.; He, X.; Lin, L.; Cao, X.; Wang, Z. L. Fully Packaged Blue Energy Harvester by Hybridizing a Rolling Triboelectric Nanogenerator and an Electromagnetic Generator. *ACS Nano* **2016**, *10*, 11369−11376.
(4) Tollefson, J. Power from the Oceans: Blue Energy. *Nature* **2014**, *508*, 302−304.
(5) Schiermeier, Q.; Tollefson, J.; Scully, T.; et al. Energy alternatives: Electricity without Carbon. *Nature* **2008**, *454*, 816−823.
(6) Scruggs, J.; Jacob, P. Harvesting Ocean Wave Energy. *Science* **2009**, *323*, 1176−1178.
(7) Xu, L.; Jiang, T.; Lin, P.; Shao, J. J.; He, C.; Zhong, W.; Chen, X. Y.; Wang, Z. L. Coupled Triboelectric Nanogenerator Networks for Efficient Water Wave Energy Harvesting. *ACS Nano* **2018**, *12*, 1849−1858.
(8) Falcão, A. F. d. O. Wave Energy Utilization: A Review of the Technologies. *Renewable Sustainable Energy Rev.* **2010**, *14*, 899−918.
(9) Wang, Z. L.; Jiang, T.; Xu, L. Toward the Blue Energy Dream by Triboelectric Nanogenerator Networks. *Nano Energy* **2017**, *39*, 9−23.
(10) Xu, M.; Wang, S.; Zhang, S. L.; Ding, W.; Kien, P. T.; Wang, C.; Li, Z.; Pan, X.; Wang, Z. L. A Highly-Sensitive Wave Sensor Based on Liquid-Solid Interfacing Triboelectric Nanogenerator for Smart Marine Equipment. *Nano Energy* **2019**, *57*, 574.
(11) Ahmed, A.; Saadatnia, Z.; Hassan, I.; Zi, Y.; Xi, Y.; He, X.; Zu, J.; Wang, Z. L. Self-Powered Wireless Sensor Node Enabled by a Duck-Shaped Triboelectric Nanogenerator for Harvesting Water Wave Energy. *Adv. Energy Mater.* **2017**, *7*, 1601705.
(12) Chen, J.; Guo, H.; Liu, G.; Wang, X.; Xi, Y.; Javed, M. S.; Hu, C. A Fully-Packaged and Robust Hybridized Generator for Harvesting Vertical Rotation Energy in Broad Frequency Band and Building up Self-Powered Wireless Systems. *Nano Energy* **2017**, *33*, 508−514.
(13) Kurt, E.; Cottone, F.; Uzun, Y.; Orfei, F.; Mattarelli, M.; Özhan, D. Design and Implementation of a New Contactless Triple Piezoelectrics Wind Energy Harvester. *Int. J. Hydrogen Energy* **2017**, *42*, 17813−17822.
(14) Li, D.; Wu, Y.; Da Ronch, A.; Xiang, J. Energy Harvesting by Means of Flow-Induced Vibrations on Aerospace Vehicles. *Prog. Aeronaut. Sci.* **2016**, *86*, 28−62.
(15) Wang, J.; Wu, C.; Dai, Y.; Zhao, Z.; Wang, A.; Zhang, T.; Wang, Z. L. Achieving Ultrahigh Triboelectric Charge Density for Efficient Energy Harvesting. *Nat. Commun.* **2017**, *8*, 88.
(16) Shi, Q.; Wang, H.; Wu, H.; Lee, C. Self-Powered Triboelectric Nanogenerator Buoy Ball for Applications Ranging from Environment Monitoring to Water Wave Energy Farm. *Nano Energy* **2017**, *40*, 203−213.
(17) Rodrigues, C. R. S.; Alves, C. A. S.; Puga, J.; Pereira, A. M.; Ventura, J. O. Triboelectric Driven Turbine to Generate Electricity from the Motion of Water. *Nano Energy* **2016**, *30*, 379−386.
(18) Wang, Z. L. Triboelectric Nanogenerators as New Energy Technology and Self-Powered Sensors - Principles, Problems and Perspectives. *Faraday Discuss.* **2014**, *176*, 447−58.
(19) Zhang, S. L.; Xu, M.; Zhang, C.; Wang, Y.-C.; Zou, H.; He, X.; Wang, Z.; Wang, Z. L. Rationally Designed Sea Snake Structure Based Triboelectric Nanogenerators for Effectively and Efficiently Harvesting Ocean Wave Energy with Minimized Water Screening Effect. *Nano Energy* **2018**, *48*, 421−429.
(20) Xu, M.; Wang, P.; Wang, Y.-C.; Zhang, S. L.; Wang, A. C.; Zhang, C.; Wang, Z.; Pan, X.; Wang, Z. L. A Soft and Robust Spring Based Triboelectric Nanogenerator for Harvesting Arbitrary Directional Vibration Energy and Self-Powered Vibration Sensing. *Adv. Energy Mater.* **2018**, *8*, 1702432.
(21) Zhao, X. J.; Tian, J. J.; Kuang, S. Y.; Ouyang, H.; Yan, L.; Wang, Z. L.; Li, Z.; Zhu, G. Biocide-Free Antifouling on Insulating Surface by Wave-Driven Triboelectrification-Induced Potential Oscillation. *Adv. Mater. Interfaces* **2016**, *3*, 1600187.
(22) Wang, Z. L. On Maxwell's Displacement Current for Energy and Sensors: The Origin of Nanogenerators. *Mater. Today* **2017**, *20*, 74−82.
(23) Wen, Z.; Guo, H.; Zi, Y.; Yeh, M. H.; Wang, X.; Deng, J.; Wang, J.; Li, S.; Hu, C.; Zhu, L.; Wang, Z. L. Harvesting Broad Frequency Band Blue Energy by a Triboelectric-Electromagnetic Hybrid Nanogenerator. *ACS Nano* **2016**, *10*, 6526−34.
(24) Chen, J.; Yang, J.; Li, Z.; Fan, X.; Zi, Y.; Jing, Q.; Guo, H.; Wen, Z.; Pradel, K. C.; Niu, S.; Wang, Z. L. Networks of Triboelectric Nanogenerators for Harvesting Water Wave Energy: A Potential Approach Toward Blue Energy. *ACS Nano* **2015**, *9*, 3324−31.
(25) Jiang, T.; Yao, Y.; Xu, L.; Zhang, L.; Xiao, T.; Wang, Z. L. Spring-Assisted Triboelectric Nanogenerator for Efficiently Harvesting Water Wave Energy. *Nano Energy* **2017**, *31*, 560−567.
(26) Shao, H.; Wen, Z.; Cheng, P.; Sun, N.; Shen, Q.; Zhou, C.; Peng, M.; Yang, Y.; Xie, X.; Sun, X. Multifunctional Power Unit by Hybridizing Contact-Separate Triboelectric Nanogenerator, Electromagnetic Generator and Solar Cell for Harvesting Blue Energy. *Nano Energy* **2017**, *39*, 608−615.
(27) Zhu, G.; Su, Y. J.; Bai, P.; Chen, J.; Jing, Q. S.; Yang, W. Q.; Wang, Z. L. Harvesting Water Wave Energy by Asymmetric Screening of Electrostatic Charges on a Nanostructured Hydrophobic Thin-Film Surface. *ACS Nano* **2014**, *8*, 6031−6037.
(28) Su, Y. J.; Wen, X. N.; Zhu, G.; Yang, J.; Chen, J.; Bai, P.; Wu, Z. M.; Jiang, Y. D.; Wang, Z. L. Hybrid Triboelectric Nanogenerator for Harvesting Water Wave Energy and as a Self-Powered Distress Signal Emitter. *Nano Energy* **2014**, *9*, 186−195.
(29) Xu, L.; Pang, Y. K.; Zhang, C.; Jiang, T.; Chen, X. Y.; Luo, J. J.; Tang, W.; Cao, X.; Wang, Z. L. Integrated Triboelectric Nanogenerator Array Based on Air-Driven Membrane Structures for Water Wave Energy Harvesting. *Nano Energy* **2017**, *31*, 351−358.
(30) Lin, Z. H.; Cheng, G.; Li, X. H.; Yang, P. K.; Wen, X. N.; Wang, Z. L. A Multi-Layered Interdigitative-Electrodes-Based Triboelectric Nanogenerator for Harvesting Hydropower. *Nano Energy* **2015**, *15*, 256−265.
(31) Zhao, L.; Zheng, Q.; Ouyang, H.; Li, H.; Yan, L.; Shi, B.; Li, Z. A Size-Unlimited Surface Microstructure Modification Method for Achieving High Performance Triboelectric Nanogenerator. *Nano Energy* **2016**, *28*, 172−178.
(32) Wen, X.; Yang, W.; Jing, Q.; Wang, Z. L. Harvesting Broadband Kinetic Impact Energy from Mechanical Triggering/Vibration and Water Waves. *ACS Nano* **2014**, *8*, 7405−7412.
(33) Xu, L.; Pang, Y.; Zhang, C.; Jiang, T.; Chen, X.; Luo, J.; Tang, W.; Cao, X.; Wang, Z. L. Integrated Triboelectric Nanogenerator Array Based on Air-Driven Membrane Structures for Water Wave Energy Harvesting. *Nano Energy* **2017**, *31*, 351−358.

DOI: 10.1021/acsnano.8b08274
ACS Nano 2019, 13, 1932−1939